DALTON
FULL PAPER

Cationic 2,6-bis(imino)pyridine iron and cobalt complexes: synthesis, structures, ethylene polymerisation and ethylene/polar monomer co-polymerisation studies †

George J. P. Britovsek, Vernon C. Gibson,* Stefan K. Spitzmesser, Kilian P. Tellmann, Andrew J. P. White and David J. Williams

Department of Chemistry, Imperial College, Exhibition Road, London, UK SW7 2AY. E-mail: v.gibson@ic.ac.uk

Received 23rd July 2001, Accepted 13th December 2001
First published as an Advance Article on the web 20th February 2002

The synthesis and characterisation of a series of cationic bis(imino)pyridine iron and cobalt complexes of the type $[LMCl(D)]SbF_6$ (D = CH_3CN or thf) and $[LM(R_2acac)]SbF_6$ (R = CH_3, CF_3, Ph) are described {L = 2,6-bis[1-(2,6-diisopropylphenylimino)ethyl]pyridine, M = Fe or Co}. The solid state structures of these five-coordinate complexes vary between square-based pyramidal and trigonal bipyramidal geometries, depending on the ligands used. Attempts to synthesise cationic metal alkyl complexes of the type $[LMR]^+$ were unsuccessful. However, these complexes serve as highly active ethylene polymerisation catalysts when activated with MAO. Polymerisation activities are comparable to the activities obtained with neutral dichloride precursors $[LMCl_2]$ and the resulting polymer properties are nearly identical, suggesting that in all cases the same active species is being generated. The polymerisation activity is not inhibited by the presence of donors such as thf or CH_3CN and these cationic precursors can be activated with less co-catalyst than is normally used for neutral dichloride pre-catalysts. As little as 10 equiv. TMA, in combination with 1 equiv. $B(C_6F_5)_3$, afford a highly active polymerisation system. Co-polymerisation studies of ethylene with polar monomers such as methyl methacrylate (MMA) or styrene resulted in polymer production with high activities. However, in both cases no co-polymer is obtained. The activity of the catalyst is significantly reduced in the presence of methyl acrylate (MA) or 2-vinyl-1,3-dioxolane (VDO) and again no co-polymer is produced. Polar monomers such as vinyl acetate, acrolein and acrylonitrile deactivate the catalyst.

Introduction

During the past five years, there have been a number of significant advances in the development of olefin polymerisation catalysts. Early transition-metal Ziegler–Natta systems and chromium based catalysts, both exploited commercially over many years, have been joined recently by several families of highly active late-transition metal catalysts based, for example, on iron, cobalt and nickel.[1–3] Amongst these new systems, the bis(imino)pyridine iron and cobalt systems, discovered independently by Brookhart, Bennett and ourselves,[4–7] have attracted interest, both in academia and particularly in industry,[8,9] because of 1) their exceptionally high activities for ethylene polymerisation,[10] 2) their remarkable selectivities for ethylene oligomerisation to linear α-olefins[11,12] and 3) their suitability for adaptation to existing commercial processes. Various modifications to the original bis(imino)pyridine ligand framework have been reported, but have generally afforded less active systems.[13–21]

The increased poison resistance of late metal systems has fuelled the idea that these catalysts may be suited to the co-polymerisation of hydrocarbon olefins with polar monomers.[22] Noteworthy in this context is the work by Yamamoto from the early 1970s, who showed that related late-transition metal complexes such as $(bipy)_2FeEt_2$ are active catalysts for the homo-polymerisation of polar monomers. A range of different monomers, such as acrylonitrile (AN), methyl vinyl ketone (MVK) and methyl methacrylate (MMA) were polymerised, though generally with poor conversions.[23–25]

† Electronic supplementary data (ESI) available: the molecular structure of **4**. See: http://www.rsc.org/suppdata/dt/b1/b106614p/

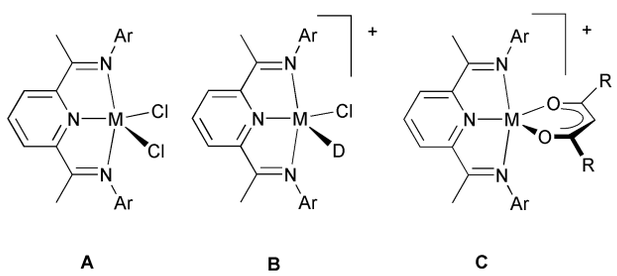

Fig. 1 Schematic representation of the dichloro (**A**), monochloro (**B**) and acac complexes (**C**) (M = Fe or Co).

Bis(imino)pyridine iron(II) and cobalt(II) dihalide complexes (**A**, Fig. 1) are commonly activated by methyl aluminoxane (MAO) or other alkyl aluminium co-catalysts.[26,27] As for other late and early transition metal systems, the exact role of MAO as a co-catalyst is not fully understood, but in general *in situ* generated cationic metal alkyl species are proposed to be the active sites in these catalyst systems. Theoretical investigations have been based on the involvement of such species in the polymerisation mechanism,[28,29] but no experimental evidence for the presence of cationic alkyl species has been obtained to date. A particular difficulty in the synthesis of well-defined cationic alkyl complexes of iron appears to be the instability of potential iron(II) dialkyl precursors.[30,31] Stable iron(II) dimethyl or diethyl compounds are rare in organo-iron chemistry, the two six-coordinate iron(II) complexes $(dmpm)_2FeMe_2$[32] and $(bipy)_2FeEt_2$[33] being the only examples that have been structurally characterised. In addition, the five-coordinate complex $(PPh_3)_3FeMe_2$ was reported by Yamamoto and co-workers to decompose above −10 °C.[34] Attempts to obtain $LFeR_2$ species *via* treatment of $LFeCl_2$ with a range of main group alkyl

reagents usually afforded the coupled R–R product, most likely *via* reductive elimination from an unstable $LFeR_2$ species. Such reactivity is well-precedented for iron(II) dialkyls.[35] Cationic alkyl derivatives based on the heavier second row metals, ruthenium and rhodium, have been synthesised recently, but their lack of polymerisation activity severely limits their usefulness in the study of the polymerisation mechanism.[36]

In order to address the co-polymerisation of hydrocarbon olefins with polar monomers it is desirable to reduce, or preferably eliminate, the requirement for an aluminium activator which makes the cationic alkyl species an important objective. We decided, therefore, to target cationic *pre-catalysts* of iron and cobalt containing bis(imino)pyridine ligands with readily displaceable co-ligands which, on the one hand, would allow problematic $LFeR_2$ to be avoided, and on the other hand, could allow access to the desired cationic mono-alkyl species *via* treatment of $LFeX^+$ with a small amount of a suitable alkylating agent or activator.

Here we describe our results on the synthesis and characterisation of cationic bis(imino)pyridine iron and cobalt complexes containing either one chloro substituent and a neutral donor D (**B**, Fig. 1) or a bidentate monoanionic acetylacetonate (acac) ligand (**C**).[37] The catalytic activity of these complexes as catalysts for the polymerisation of ethylene with MAO and other co-catalysts has been examined and compared with the neutral dichloride pre-catalysts. In addition, co-polymerisation experiments of ethylene with polar monomers have been carried out.

Results and discussion

Synthesis and characterisation of cationic complexes

Initially, dialkyl iron complexes containing bis(imino)pyridine ligands were targeted. Attempts to alkylate bis(imino)pyridine iron dichloride **1a** with Grignard reagents or alkyl lithium compounds generally yielded decomposition products, probably as a result of reductive processes.[35] The reaction between bis(imino)pyridine cobalt dichloride **1b** and 2 equiv. of MeMgCl also led to reduction, in this case to give a relatively stable bis(imino)pyridine cobalt(I) methyl complex, which is the subject of a separate report.[38]

In order to avoid potential reductive decomposition pathways available to dialkyl iron(II) species, cationic monochloro iron(II) complexes of type **B** (Fig. 1) were targeted, with the aim of generating monoalkyl iron(II) complexes therefrom. The reaction of bis(imino)pyridine iron and cobalt dichloride **1a** and **1b** with one equiv. of $AgSbF_6$ in acetonitrile or tetrahydrofuran results in the clean formation of the cationic monochloro iron and cobalt complexes, containing one acetonitrile (**2a** and **2b**) or thf ligand (**3**) coordinated to the metal centre (Scheme 1). It is interesting to note that in these complexes the acetonitrile or thf ligand occupies the apical position of the square based pyramid, in contrast to a closely related bis(2,6-iminophosphoranyl)pyridine cobalt complex reported recently.[21]

Several attempts have been made to generate a donor-free four-coordinate monochloro iron(II) complex. For example, when the reaction with $AgSbF_6$ was carried out in dichloromethane, an orange–red solid was obtained. X-Ray analysis of the crystallised product (CH_2Cl_2/pentane) revealed a five-coordinated complex **4** containing one molecule of H_2O bound in the apical position (see ESI for a Figure of this complex). The scavenging of water, which probably originated from adventitious water in the solvent, is in keeping with the rare occurrence and high reactivity of four-coordinate square planar iron(II) complexes.[39]

The second chloride ligand can be abstracted with silver acetylacetonate [Ag(acac)] to afford the donor-free iron and cobalt acac complexes of type **C** (Fig. 1). Complexes **5a** and **5b**

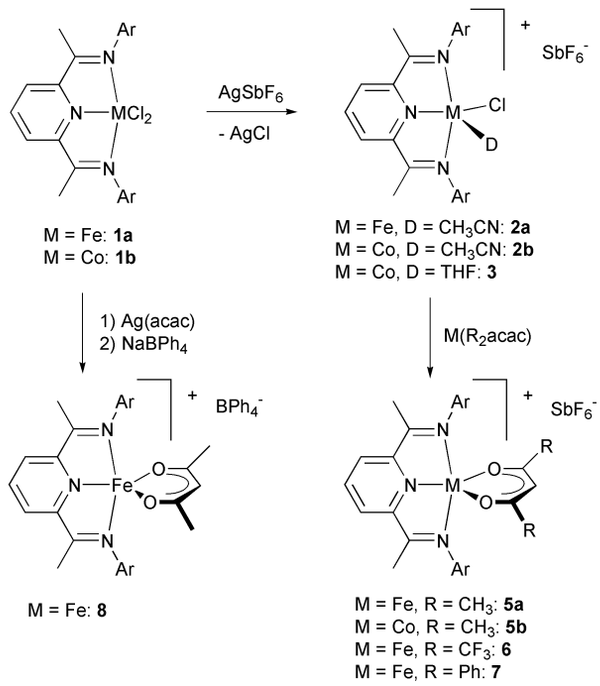

Scheme 1

can also be prepared by sequential addition of $AgSbF_6$ and Ag(acac) in acetonitrile solution in one pot, without isolating the intermediate cationic monochloride complexes. Introducing differently substituted acetylacetonates requires a slight change in the reaction procedure: silver salts of 1,3-diphenyl- and 1,3-bis(trifluoromethyl)-acetylacetonate are not commercially available and therefore sodium salts of the desired substituted acetylacetone were employed in the reaction with the monochloro complex **2a** to obtain the substituted acac complexes **6** and **7** in good yields. Other counter ions can be introduced by the addition of Ag(acac), followed by the sodium salt of the tetraphenylborate anion BPh_4^- in acetonitrile to afford complex **8**. Initial reaction of the dichloride complex **1a** with $NaBPh_4$ did not yield a cationic complex and starting material was recovered. This observation suggests the necessity for a silver reagent in at least one of the halide abstractions.

All compounds were characterised by ^1H NMR, UV/VIS and IR spectroscopy, FAB mass spectrometry, magnetic susceptibility and microanalysis. In addition, the crystal structures of complexes **2a**, **2b**, **3**, **4**, **5a**, **6** and **7** were determined by single-crystal X-ray diffraction studies.

X-Ray crystallographic analysis. Complexes **2a** and **2b** are isomorphous but with small differences in the included solvent molecules. Compounds **4** and **6** were both found to crystallise as different polymorphic forms, with monoclinic and triclinic polymorphs being observed in each case: these different polymorphs have been denoted as **4i/4ii** and **6i/6ii** respectively. The complexes fall into two distinct groups, those bearing, in addition to the tridentate 2,6-bis(imino)pyridine ligand, two monodentate substituents on the metal centre (**2a**, **2b**, **3** and **4**), and those with a bidentate ligand occupying these two sites (**5a**, **6** and **7**). Representative illustrations of the structures of compounds **2a**, **3** and **5a** are given in Figs. 2, 3 and 4. Fig. 5 provides a schematic diagram for the purpose of identifying the principal geometric and conformational features of the series of structures; comparative data relating to this figure are given in Table 1.

Compounds **2a**, **2b**, **3** and both polymorphs of **4** all have approximate molecular C_s symmetry about the X–M–Y plane that also contains the pyridyl nitrogen atom N(1) (Fig. 5). The geometry at the metal centre is, in all cases, distorted square pyramidal with the metal atom lying *ca.* 0.35 Å out of the basal

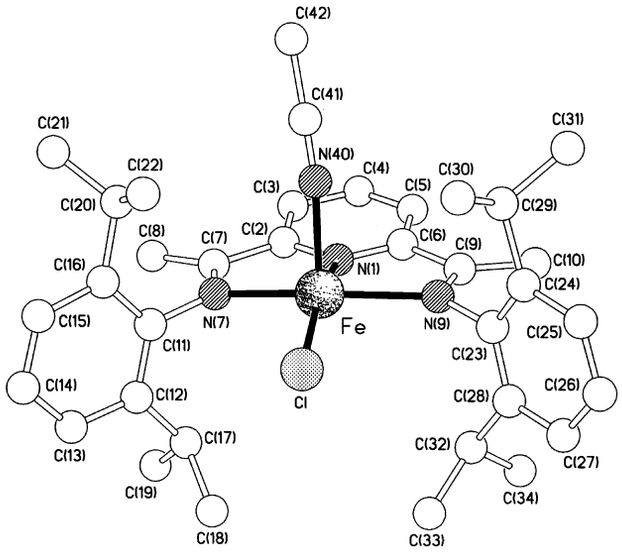

Fig. 2 The molecular structure of **2a**.

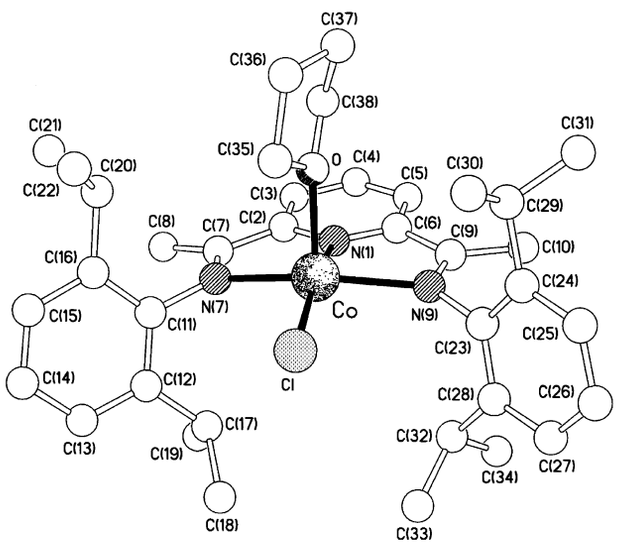

Fig. 3 The molecular structure of **3**.

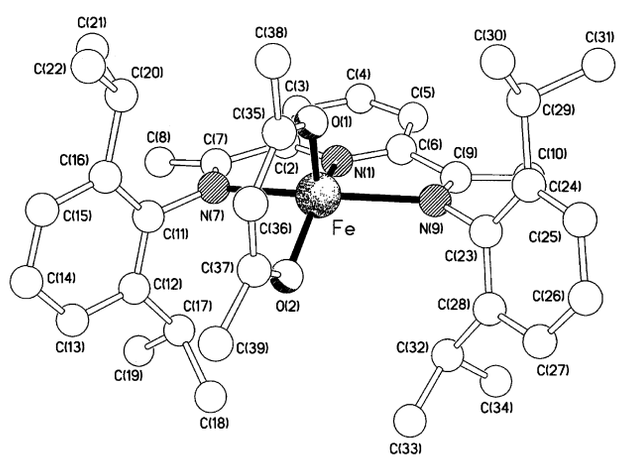

Fig. 4 The molecular structure of **5a**.

coordination plane (N_3Y) in the direction of the apical ligand X. The principal distortion from square pyramidal geometry is due to the coordination constraints of the tridentate 2,6-bis(imino)pyridine ligand which results in *trans*-basal N(7)–M–N(9) angles that are in the range 142.7(3)–145.2(3)°. The equivalent metal–nitrogen bond lengths in these five structures are, within statistical significance, the same (Table 2), with in each case that to the pyridyl nitrogen atom N(1) being shorter

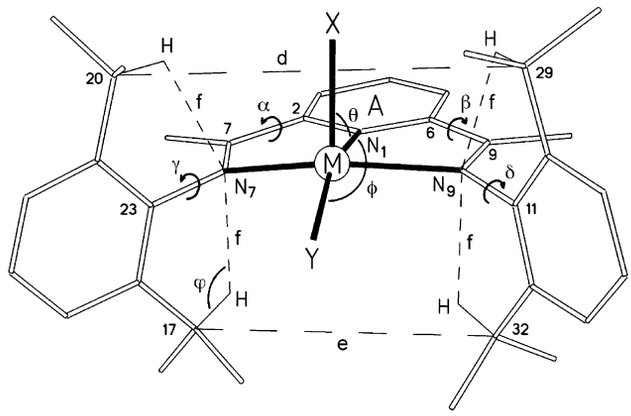

Fig. 5 Schematic diagram identifying the principal geometric and conformational parameters in structures **2a**, **2b**, **3**, **4i**, **4ii**, **5a**, **6i**, **6ii** and **7**.

than those to the imine nitrogens N(7) and N(9). The geometry and conformation of the tridentate ligands are, in each case, very similar with a retention of the double bond character for the C(7)–N(7) and C(9)–N(9) bonds, and an approximately orthogonal orientation of the two 2,6-diisopropylphenyl rings to the basal coordination plane (δ and γ in Fig. 5). This conformation is stabilised, as has been observed previously,[13,40,41] by C–H ··· N(pπ) interactions (*f* in Fig. 5). The separations of the "upper" and "lower" isopropyl carbon atoms, C(20) and C(29) [*d*], and C(17) and C(32) [*e*] respectively, expand and contract depending on the steric bulk of the apical ligand X; the most pronounced difference between the two separations is in **3** where X = thf.

The introduction of a bidentate ligand in the X and Y positions (**5a**, **6** and **7**) results in a change in the coordination geometry at the metal to one that is intermediate between square pyramidal and trigonal bipyramidal with N(7)–M–N(9) as the "trigonal" axis. The nature of the substituents on the β-diketonate moiety also has a dramatic effect on the resulting geometry of the complex. In complexes **5a** and **7** approximate molecular C_s symmetry is retained, though in **5a** there is a *ca.* 11° out of plane fold about the O(1) ··· O(2) vector of the β-diketonate ligand. In both these structures the oxygen atoms X [O(1)] and Y [O(2)] occupy, in the context of a severely distorted square pyramidal geometry, pseudo-axial and basal sites respectively with Y positioned approximately centrally between the planes of the two 2,6-diisopropylphenyl rings (Figs. 6 and 7).

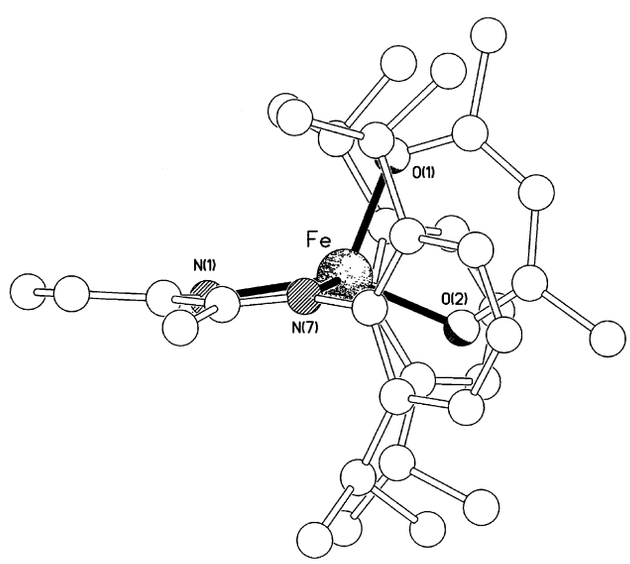

Fig. 6 View down the N(7) ··· N(9) vector of the structure of **5a** showing the distorted coordination geometry and the positioning of O(2) between the faces of the two 2,6-diisopropylphenyl rings.

Table 1 Comparative conformational and geometric parameters for compounds **2a**, **2b**, **3**, **4i**, **4ii**, **5a**, **6i**, **6ii** and **7**

	a [a]	b [a]	c [b]	θ [c]	φ [c]	ζ [d]	d [e]	e [e]	α [f]	β [f]	γ [f]	δ [f]	f [g]	ψ [h]
2a	0.35	0.01	0.46	87	161	90	7.08	5.45	7	7	89	89	2.33–2.41	109–114
2b	0.32	0.05	0.39	86	165	89	6.96	5.31	4	4	88	89	2.34–2.45	110–114
3	0.34	0.06	0.31	90	165	89	7.60	4.79	5	2	83	89	2.40–2.51	110–111
4i	0.38	0.03	0.19	86	161	86	7.00	5.43	3	3	84	89	2.39–2.43	110–112
4ii	0.34	0.06	0.36	89	164	88	7.28	5.13	3	4	89	85	2.38–2.43	111–112
5a	0.46	0.12	0.42	120	147	84	7.31	5.35	12	9	86	78	2.40–2.56	102–111
6i	0.34	0.29	−0.17	127	146	76	6.65	6.56	2	1	82	72	2.46–2.54	107–111
6ii	0.36	0.22	−0.09	127	146	77	6.70	6.50	2	2	83	74	2.46–2.54	107–110
7	0.49	0.11	0.28	122	147	89	6.91	5.49	5	6	82	84	2.42–2.50	106–112

[a] a is the deviation (Å) of the metal atom from the N_3Y plane, which is planar to within b Å. [b] c is the displacement of the metal atom out of the plane of the pyridyl ring A towards X, a negative value indicates that the metal lies below this plane. [c] θ and φ are the N(1)–M–X and N(1)–M–Y angles (°), respectively. [d] ζ is the dihedral angle (°) between the MN_3 and MXY planes. [e] d and e are the separations (Å) of the isopropyl carbon atoms C(20) and C(29), and C(17) and C(32), respectively. [f] α, β, γ and δ are the mean torsional twists (°) about the C(2)–C(7), C(6)–C(9), N(7)–C(11) and N(9)–C(23) bonds, respectively. [g] f is the range (Å) for the isopropyl methine hydrogen H ··· N distances. [h] ψ is the range (°) of C–H ··· N angles for the contact f.

Table 2 Comparative selected bond lengths (Å) and angles (°) for compounds **2a**, **2b**, **3**, **4i**, **4ii**, **5a**, **6i**, **6ii** and **7**

	2a [a]	**2b** [b]	**3** [c]	**4i** [d]	**4ii** [d]	**5a** [e]	**6i** [e]	**6ii** [e]	**7** [e]
M–X	2.109(12)	2.049(11)	2.079(4)	2.121(6)	2.070(8)	1.960(5)	2.026(5)	2.027(7)	1.959(3)
M–Y	2.231(3)	2.218(3)	2.228(1)	2.230(3)	2.237(3)	1.940(4)	2.006(5)	2.015(6)	1.960(3)
M–N(1)	2.110(7)	2.052(8)	2.056(4)	2.072(8)	2.092(7)	2.101(5)	2.102(6)	2.109(7)	2.109(4)
M–N(7)	2.221(8)	2.188(8)	2.205(4)	2.217(7)	2.222(7)	2.247(5)	2.222(6)	2.220(7)	2.205(4)
M–N(9)	2.223(8)	2.174(9)	2.171(3)	2.227(7)	2.210(7)	2.211(6)	2.230(6)	2.223(7)	2.201(4)
C(7)–N(7)	1.275(12)	1.259(13)	1.285(6)	1.274(12)	1.284(12)	1.274(9)	1.287(10)	1.297(11)	1.279(6)
C(9)–N(9)	1.283(12)	1.281(14)	1.289(6)	1.236(11)	1.286(12)	1.261(9)	1.285(10)	1.280(11)	1.275(6)
X–M–Y	112.3(3)	109.4(3)	105.3(2)	112.5(2)	107.1(3)	92.0(2)	87.3(2)	86.7(3)	90.9(1)
X–M–N(1)	87.0(3)	85.9(4)	89.6(2)	85.7(3)	88.6(3)	120.3(2)	126.5(2)	127.0(3)	122.3(1)
X–M–N(7)	94.9(3)	95.8(3)	98.9(2)	99.8(2)	98.7(3)	104.5(2)	106.1(2)	106.7(3)	105.4(1)
X–M–N(9)	95.3(4)	97.2(4)	97.8(2)	93.5(2)	96.4(3)	101.1(2)	90.3(2)	91.7(3)	102.7(1)
Y–M–N(1)	160.7(3)	164.6(3)	165.1(1)	161.2(2)	164.2(2)	146.8(2)	145.7(2)	145.9(3)	146.8(1)
Y–M–N(7)	103.6(2)	102.6(2)	103.2(1)	106.4(2)	105.4(2)	93.2(2)	93.4(2)	93.9(3)	101.0(1)
Y–M–N(9)	104.1(2)	103.2(2)	101.9(1)	100.2(2)	101.8(2)	109.8(2)	116.5(2)	114.9(3)	100.6(1)
N(1)–M–N(7)	73.2(3)	75.1(3)	74.4(1)	73.3(3)	73.3(3)	72.8(2)	73.3(2)	73.6(3)	73.0(1)
N(1)–M–N(9)	73.0(3)	73.9(3)	75.0(1)	73.1(3)	73.8(3)	73.5(2)	73.8(2)	73.3(3)	73.1(1)
N(7)–M–N(9)	144.1(3)	145.2(3)	144.8(1)	142.7(3)	143.2(3)	144.8(2)	146.8(2)	146.8(3)	144.0(1)

[a] M = Fe, X = N(40), Y = Cl. [b] M = Co, X = N(40), Y = Cl. [c] M = Co, X = O, Y = Cl. [d] M = Fe, X = O(1), Y = Cl. [e] M = Fe, X = O(1), Y = O(2).

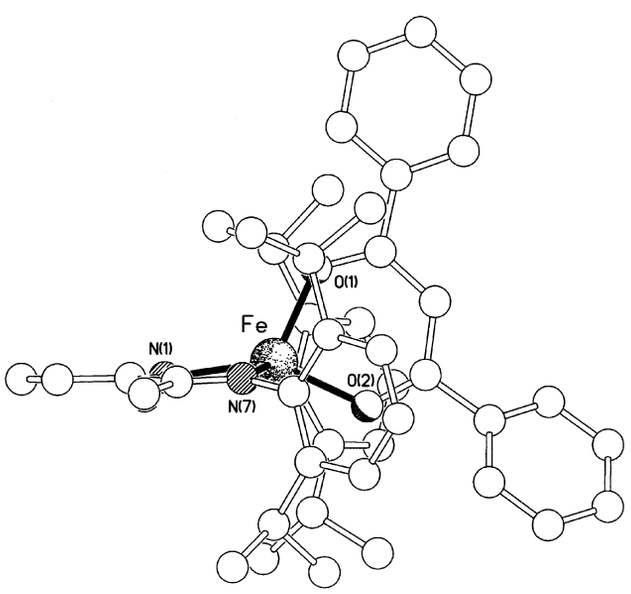

Fig. 7 View down the N(7) ··· N(9) vector of the structure of **7** showing the distorted coordination geometry and the positioning of O(2) between the faces of the two 2,6-diisopropylphenyl rings, compare with Fig. 6.

By contrast, the two polymorphs of compound **6**, with CF_3 substituents on the β-diketonate ligand, both adopt a geometry with near C_2 symmetry about the Fe–N(1) axis, the X–M–Y plane [O(1)–Fe–O(2)] being twisted about this vector by *ca.* 76° to the "basal" N_3M plane *cf.* 84 and 89° in **5a** and **7** respectively. Furthermore, the metal atom in **6i** and **6ii** lies slightly "below" the plane of the pyridyl ring, whereas in each of the other seven complexes it is positioned significantly "above" (Table 1). This geometry is also highlighted by the increase in the X–M–N(1) angle θ, and is particularly well illustrated in Fig. 8 when compared with those in Fig. 6 and 7. The Fe–N bond distances are unchanged from those observed for **2a**, **4i** and **4ii**, as are the C=N double bond lengths. In **5a** and **7** the Fe–O distances are all effectively the same (av. 1.955 Å) but those in **6i** and **6ii** are noticeably longer (av. 2.019 Å), there being no differentiation between pseudo-axial and basal Fe–O bonds. Both polymorphs of **6** also exhibit larger differences in the torsional twists δ and γ of the 2,6-diisopropylphenyl rings out of the N_3M coordination plane than those observed in the other complexes, and have very much closer to equal isopropyl ··· isopropyl separations d and e (Fig. 5 and Table 1).

The packing of the molecules in **2a**, **2b** and **3** is similar with, in each case, a pseudo-layer structure being formed based on a co-alignment of the basal coordination planes, but with no intermolecular interactions of note. In **4i** there are intermolecular O–H ··· F hydrogen bonds [2.74 and 2.87 Å] between the apical aqua ligand and the SbF_6 anion, a pseudo-dimer being formed involving a centrosymmetrically related pair of complex cations and SbF_6 anions. In **4ii** there is only a single cation ··· anion O–H ··· F hydrogen bond [2.81 Å]. There are no intermolecular packing interactions of note in complex **5a**, the SbF_6 anion being disordered. Both polymorphs

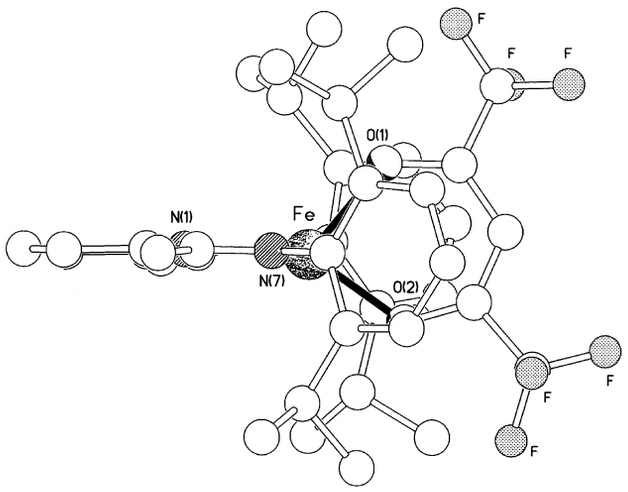

Fig. 8 View down the N(7) ··· N(9) vector of the structure of **6** showing the pseudo-trigonal bipyramidal geometry at iron, the positioning of the iron atom "below" the plane of the pyridyl ring and the sandwiching of the β-diketonate chelate ring between the faces of the two 2,6-diisopropylphenyl rings.

of **6** exhibit an unusual juxtaposition of the cations and anions with, in each case, one of the fluorine atoms of the ordered SbF_6 anion being positioned proximal to the iron centre in the vacant "octahedral" coordination site (Fig. 9). It should be

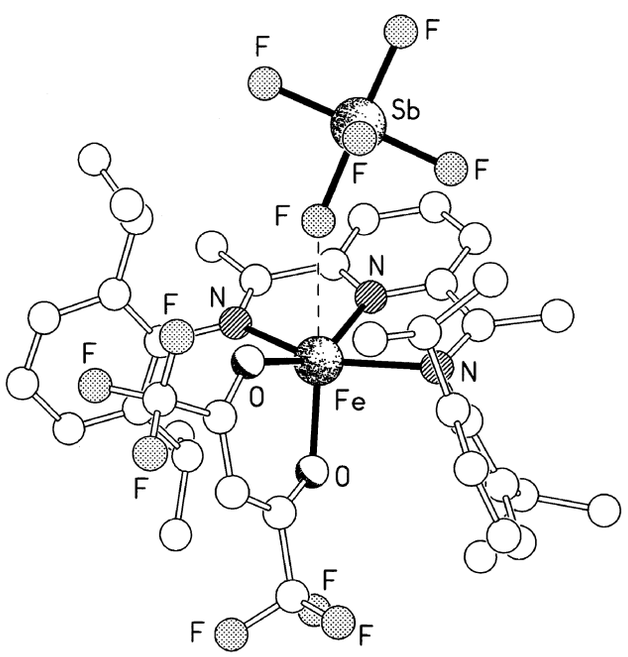

Fig. 9 The approach of one of the SbF_6 fluorine atoms to the vacant "octahedral" site of the iron centre in **6**.

noted that previous attempts to synthesis six-coordinate bis(imino)pyridine iron(II) complexes of the type $LFeCl_2(D)$ (where D = CO, $P(OMe)_3$, PMe_3) systematically failed and that this is the first indication of a tendency towards octahedral coordination in these five-coordinate complexes. In **6i** and **6ii** the F ··· Fe separations are 2.70 and 2.77 Å respectively, with O(1)–Fe ··· F angles of 159 and 160°. This distance is significantly longer than the Fe–F bond between the iron atom and a fluorine atom of the SbF_6 anion in, for example, (hexafluoroantimonate)(*meso*-tetraphenylporphinato)iron(III) [*ca.* 2.11 Å].[42] However, the Cambridge Crystallographic Database (version 5.20) reveals only one example of a non-bonded Fe ··· F contact of less than 3.3 Å occurring between a five-coordinate iron centre and a fluorine atom (3.24 Å).[43] The aforementioned close positioning of the anion and cation in **6i** and **6ii** also favours the formation of two weak F ··· π contacts to the pyridyl ring; in **6i** these separations are both 3.14 Å, whilst in **6ii** they are 3.12 and 3.38 Å. In **7**, however, there are no such approaches, and the shortest Fe ··· F separation is 3.78 Å.

Magnetic susceptibility. All of the described complexes are paramagnetic. Their magnetic moments were determined by the Evans' NMR method (see Experimental section).[44–47] The Fe(II) complexes afford magnetic moments between 5.0 and 5.4 μ_B, consistent with four unpaired electrons and a quintet ground state for the iron(II) centres. The magnetic moments for the cobalt(II) complexes are around 4.6 μ_B, suggesting a quartet spin state with three unpaired electrons for the Co(II) centres. Evidently, replacing a chloride ligand by ligands that exert a stronger ligand field, such as CH_3CN, thf or acac, does not affect the high-spin configuration of the metal centres.

^{1}H NMR spectroscopy. Despite the paramagnetic nature of the cationic complexes, ^{1}H NMR spectra can be obtained. All signals appear as broad singlets and assignments of the resonances can be made on the basis of integration, proximity to the paramagnetic metal centre and by comparison with similar paramagnetic complexes.[10] For some proton signals, dramatic differences in chemical shifts are observed between the neutral dihalide precursors and the cationic complexes. In Fig. 10 the ^{1}H

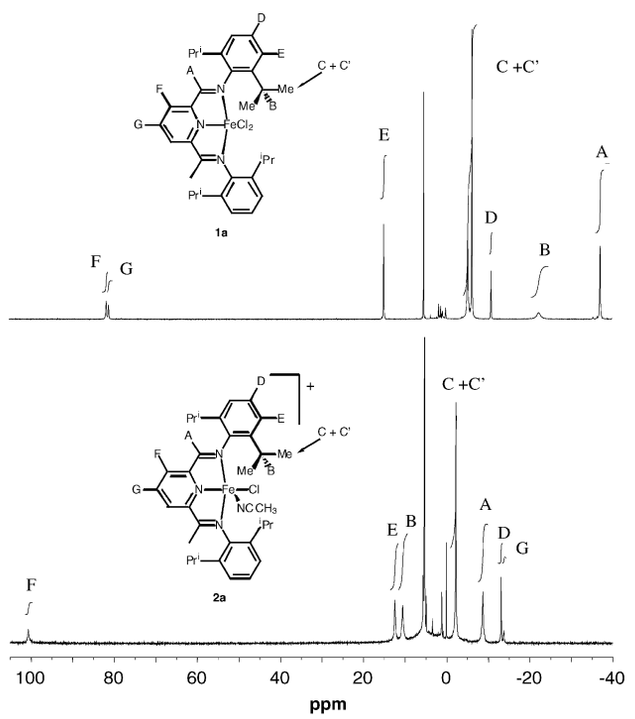

Fig. 10 ^{1}H NMR spectra of complexes **1a** and **2a**.

NMR spectrum of complex **2a** is shown, together with the parent dichloride precursor **1a**. From these spectra it can be seen that for both complexes, the *meta*-pyridyl protons (F) of the ligand are found downfield at 90–100 ppm, which is indeed common for most iron bis(iminopyridine) complexes. In sharp contrast, the *para*-pyridyl proton (G), which is found at 83 ppm in **1a**, appears considerably further upfield in the case of the cationic complexes, *e.g.* at about −14 ppm for **2a** and −33 ppm for **5a**. The backbone methyls (A) are also strongly affected, but their shifts are not easily rationalised, *e.g.* −37 ppm (**1a**), −8 ppm (**2a**) and −61 ppm (**5a**). The aromatic protons (D and E) and the isopropyl methyl groups (C, C′), which are further removed from the iron centre, are largely unaffected. In some cases not all of the expected signals are observed, for example the methyl groups of the CH_3CN ligand in **1a** and **1b** and the

thf signals in **3** are not observed. This may be due to exchange processes or fluxional behaviour, resulting in an increased broadening of these signals.

UV/VIS Spectroscopy. All the iron and cobalt complexes presented here are intensely coloured and, upon activation of the pre-catalysts with the co-catalyst MAO, dramatic colour changes are observed. For example, solutions of the bis(imino)pyridine iron dichloride complex **1a** are blue, whereas the monochloride **2a** and acac iron complexes (**5a**, **6**, **7**) are red, all of which turn orange after addition of MAO. The cobalt analogues are green and change to purple upon activation. UV/VIS spectroscopic studies of MAO-activated olefin polymerisation systems have been carried out previously for metallocenes and α-diimine nickel catalysts.[48–50]

The UV/VIS spectra of the dichloride (**1a**, **1b**), monochloride (**2a**, **2b**) and acac (**5a**, **5b**) iron and cobalt complexes as well as the activated solutions have been recorded and are presented in Fig. 11. All iron and cobalt complexes, as well as the free ligand, show two characteristic absorptions in the UV region between 224–234 nm (ε = 27000–45000 dm^3 mol^{-1} cm^{-1}) and 280–300 nm (ε = 7000–14000 dm^3 mol^{-1} cm^{-1}) which are due to ligand based transitions (π–π*). In the visible region, the iron dichloride complex **1a** displays a broad absorption around 700 nm (ε = 2500 dm^3 mol^{-1} cm^{-1}) which is probably due to metal to ligand charge transfer (MLCT). This absorption is observed at 500–600 nm (ε = 400–600 dm^3 mol^{-1} cm^{-1}) for the iron monochloro (**2a**) and acac (**5a**) complexes, and is considered responsible for the blue (**1a**) and red (**2a** and **5a**) colours respectively.[51,52] The cobalt dichloro complex (**1b**) also shows an absorption at 700 nm, though much less intense compared to the iron analogue, and which is shifted only slightly to 650 nm for the monochloro complex (**2b**) and to 670 nm for the acac complex (**5b**). Because of its low intensity (ε = 100–200 dm^{3}mol^{-1}cm^{-1}), we believe that this absorption more likely results from a d–d transition. In addition, absorptions around 430 nm in the case of **1b** and **2b** and 480 nm (**5b**) are observed (ε = 700–900 dm^3 mol^{-1} cm^{-1}), most probably due to MLCT.

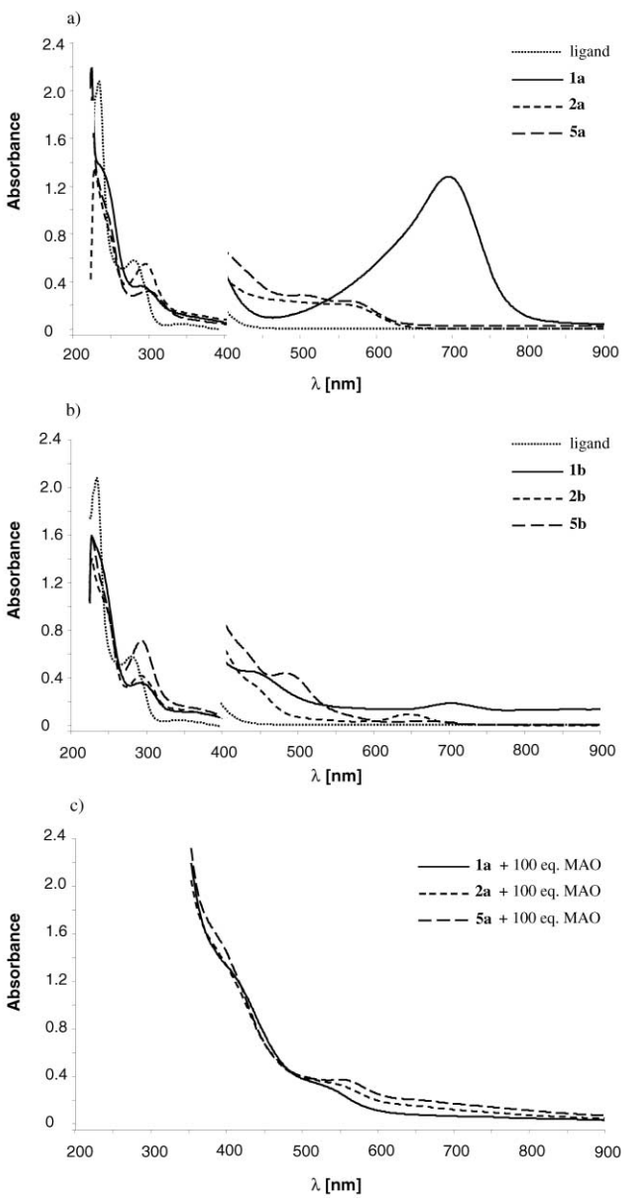

Fig. 11 UV/VIS spectra of (a) ligand and iron complexes **1a**, **2a** and **5a** (CH_2Cl_2, $c = 0.5 \times 10^{-4}$ M for 200–400 nm, $c = 5.0 \times 10^{-4}$ M for 400–900 nm), (b) ligand and cobalt complexes **1b**, **2b** and **5b** (CH_2Cl_2, $c = 0.5 \times 10^{-4}$ M for 200–400 nm, $c = 5.0 \times 10^{-4}$ M for 400–900 nm) and (c) iron complexes **1a**, **2a** and **5a** + MAO (100 equiv.) (toluene, $c = 10^{-3}$ M).

Addition of MAO activator to toluene solutions of the iron pre-catalysts **1a**, **2a** or **5a** results in all cases in a clear orange–yellow solution. These solutions display a similar, rather featureless UV/VIS spectrum (Fig. 11c), which shows that, irrespective of the pre-catalyst employed (**1a**, **2a** or **5a**) the same active species appears to be generated upon activation with MAO. This suggests that the role of MAO is possibly twofold: 1) abstraction of one chloride from a dichloride precursor and 2) an exchange reaction of the remaining chloride (or acac) ligand by an aluminium alkyl species, to generate the active metal alkyl species (see Scheme 2). As mentioned previously, alkylation of cobalt(II) precursors leads to a reduction of the metal centre to Co(I).[38] There is strong spectroscopic evidence that reduction also occurs upon activation with MAO; these studies will be reported separately in due course.

Infrared spectroscopy. All of the complexes afford characteristic absorptions for the bis(imino)pyridine ligands. The C=N stretching mode ν(C=N) is observed at 1610–1630 cm^{-1} for the coordinated bis(imino)pyridine ligand, which compares with ν(C=N) in the range of 1640 to 1645 cm^{-1} for the free ligand.[53] This shift to lower wavenumber upon complexation to a metal is consistent with observations for other 2,6-bis(imino)-pyridine metal complexes.[54–56] Two strong absorption bands between 1520 and 1580 cm^{-1} can be attributed to the combinational stretching modes (ν(C=C) + ν(C=O)) of the C=C and the C=O stretches of the coordinated acetylacetonate ligand.[54,57–59] Complex **6** shows two strong absorptions at 1206 and 1147 cm^{-1} which can be attributed to the C–F stretching mode, indicating the presence of the trifluoromethyl acetylacetonate moiety.[53,60] The characteristic absorption for the Sb–F stretching mode ν(Sb–F) is observed at *ca.* 660 cm^{-1}.[61]

Polymerisation results

Polymerisation tests with MAO as co-catalyst. Treatment of the cationic Fe complexes **2a** and **5a** with 100 equiv. MAO results in the formation of an orange–yellow solution (purple for the Co complexes **2b** and **5b**), the same colour that is observed after addition of MAO to a toluene solution of the dichloride precursors **1a** (**1b** for Co). The results in Table 3 show that both in the case of iron as well as for cobalt, similar activities for the polymerisation of ethylene are obtained for the dichloride (**1a**,**b**), monochloride (**2a**,**b**) and acac (**5a**,**b**) pre-catalysts. The polymer properties are also comparable. These polymerisation results, combined with the UV/VIS studies presented above, suggest that the same active species is being generated, irrespective of the pre-catalyst used (see Scheme 2) and that this species does not have any halide or acac ligands attached.

A significant observation is that the presence of one equivalent of a relatively strong donor such as acetonitrile does not inhibit the polymerisation reaction. We believe that both the

Table 3 Results of ethylene polymerisation with precatalysts **1a**,**b**, **2a**,**b** and **5a**,**b** in a 1 L autoclave[a]

Run	Precatalyst/ μmol	Yield/g	Activity[b]	M_w[c]	M_n[c]	M_w/M_n[c]	M_{pk}[c]	Saturated chain ends[d]	Unsaturated chain ends[d]
1	**1a** (0.5)	9.6	4800	500000	53000	9.5	285000	Polymer insoluble	
2[e,f]	**1b** (0.6)	3.7	450	14000	4200	3.3	12000	2.4	1.9
3	**2a** (0.5)	12.2	6100	278000	64000	4.3	254000	0.4	0.1
4[f]	**2b** (0.6)	1.3	220	12000	4500	2.6	8900	3.8	2.8
5	**5a** (0.5)	14.9	7500	317000	78000	4.1	179000	0.3	0.1
6[f]	**5b** (0.6)	1.2	200	12000	4600	2.7	9100	2.8	2.6

[a] General conditions: isobutane solvent, triisobutylaluminium scavenger, 100 equiv. MAO, 4 bar ethylene pressure, 50 °C, reaction time 1 hour. [b] g $mmol^{-1}$ h^{-1} bar^{-1}. [c] Determined by GPC at 135 °C. [d] Results from ^1H NMR analysis, given per 1000 carbon atoms. [e] See ref. 10. [f] 10 bar ethylene pressure.

Table 4 Results of ethylene polymerisation with precatalysts in 500 ml Fisher–Porter bottles[a]

Run	Precatalyst/ μmol	Yield/g	Activity[b]	M_w[c]	M_n[c]	M_w/M_n[c]	M_{pk}[c]	Saturated chain ends[d]	Unsaturated chain ends[d]
7	**1a** (2.0)	28.6	11400	169000	46000	3.7	87000	0.3	0.3
8	**1b** (10.0)	18.0	1400	15000	6300	2.3	13000	2.8	2.2
9	**2a** (2.0)	12.1	4840	112000	33000	3.4	82000	0.5	0.4
10	**2b** (10.0)	10.1	810	19000	7200	2.6	13000	2.0	2.1
11	**5a** (2.0)	13.4	5360	136000	52000	2.6	102000	0.5	0.4
12	**5b** (10.0)	20.9	1670	16000	5900	2.7	13000	2.2	2.2
13	**6** (2.0)	20.2	8080	146000	40000	3.6	84000	0.5	0.4
14	**7** (2.0)	18.4	7360	121000	40000	3.0	79000	0.5	0.4
15	**8** (2.0)	14.2	5680	198000	49000	4.1	111000	0.5	0.4

[a] General conditions: toluene solvent (250 ml), 100 equiv. MAO, 5 bar ethylene pressure, r.t., reaction time 15 min. [b] g $mmol^{-1}$ h^{-1} bar^{-1}. [c] Determined by GPC at 135 °C. [d] Results from ^1H NMR analysis, given per 1000 carbon atoms.

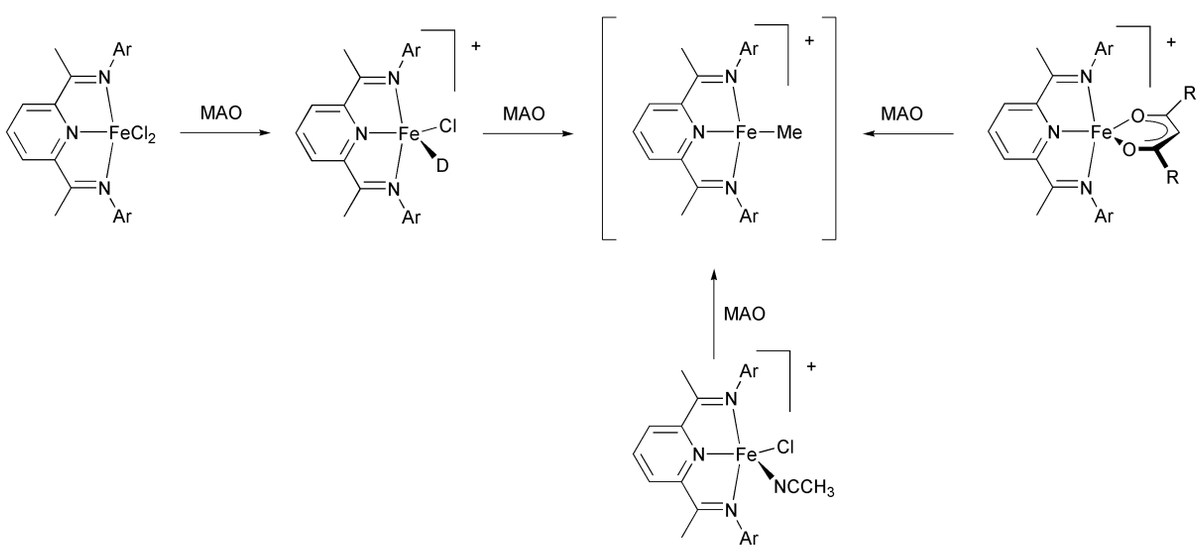

Scheme 2

acetonitrile ligand and the acac ligand are sequestered by the co-catalyst upon generation of the active species. This is further supported by the polymerisation results from Fisher–Porter glass reaction vessels at 5 bar ethylene pressure. These experiments were carried out to evaluate the influence of different acac substituents and a different counter ion (BPh_4^- in complex **8**). The results in Table 4 again show very similar activities and polymer properties for all cationic iron acac complexes **5a**–**b** and **6**–**8**. This observation suggests little interaction of the acac moiety with the active species after activation with MAO. Furthermore, no deleterious effect of the counterion is observed. The higher activity of the neutral dichloride iron pre-catalysts **1a** and **1b** compared to their cationic counterparts under these conditions is probably due to a higher initial activity within the first few minutes after activation. This leads to a higher averaged activity when shorter run times of 15 min are employed (compare runs 1–4 in Table 3 *vs.* runs 7–10 in Table 4).

The cationic cobalt complexes **2b** and **5b** also produce polyethylene with very similar activities and nearly identical molecular weight parameters compared to the dichloride pre-catalyst **1b** when tested both at 10 bar and at 5 bar ethylene pressure. This confirms that for both iron and cobalt bis(imino)pyridine complexes, the nature of the pre-catalyst—neutral or cationic—has no influence on the activity and molecular weight parameters in combination with MAO activator. From this observation we may conclude that the same active species is formed upon activation with MAO.

Polymerisation tests with co-catalysts other than MAO. Although MAO is the most frequently used activator for olefin polymerisation catalysts, the reaction steps that lead to the active species are still not adequately understood. Despite the excellent properties of MAO as a co-catalyst, this lack of understanding, combined with high cost and the fact that often

Table 5 Results of ethylene polymerisation with precatalysts **1**–**8** in Schlenk-line tests[a]

Run	Precatalyst µmol	Yield/g	Activity[b]	M_w[c]	M_n[c]	M_w/M_n[c]	M_{pk}[c] Peak 1	M_{pk}[c] Peak 2	Saturated chain ends[d]	Unsaturated chain ends[d]
16[e]	**1a** (9.4)	5.4[h]	2300	72000	6000	12.1	1100	43000	3.7	0.4
17[f]	**1a** (9.2)	1.6	700	101000	9500	10.7	2200	82000	2.5	0.2
18[e]	**1b** (9.8)	4.8	1960	17000	6700	2.5		12000	2.4	2.1
19[f]	**1b** (14.2)	1.2	340	26000	21000	2.5		23000	2.4	1.9
20[e]	**2a** (9.8)	4.9	2000	55000	6500	8.5	1200	27000	4.0	0.7
21[f]	**2a** (9.5)	1.2	510	477000	155000	3.1		511000	0.5	0
22[e]	**5a** (9.6)	4.9	2040	52000	5500	9.5	1000	20000	4.8	0.7
23[f]	**5a** (9.4)	2.6	1110	117000	40000	2.9		88000	0.5	0.4
24[g]	**5a** (10.2)	0.2	80	267000	109000	2.5		249000	1.5	0
25[e]	**5b** (9.8)	4.3	1760	19000	7300	2.6		13000	2.2	1.9
26[f]	**5b** (10.7)	1.1	410	28000	12000	2.3		21000	1.5	1.2
27[g]	**5b** (9.1)	1.0	440	23000	10000	2.3		19000	2.0	1.5
28[e]	**6** (10.2)	5.1[h]	2000	65000	5300	12.2	900	26000	4.0	0.6
29[f]	**6** (9.4)	3.1	1310	136000	44000	3.1		97000	0.9	0.3
30[e]	**7** (9.8)	5.6[h]	2290	107000	8100	13.3	900	58000	2.7	0.3
31[f]	**7** (9.8)	2.8	1140	114000	39000	3.0		84000	0.6	0.3
32[e]	**8** (10.0)	5.6[h]	2240	43000	4300	10.1	800	14000	5.9	1.4
33[f]	**8** (9.6)	2.7	1130	82000	19000	4.3		59000	1.5	0.4

[a] General conditions: toluene solvent (100 ml), 1 bar ethylene pressure, r.t. [b] g mmol^{-1} h^{-1} bar^{-1}. [c] Determined by GPC at 135 °C. [d] Results from ^{1}H NMR analysis, given per 1000 carbon atoms. [e] 100 equiv. MAO, reaction time 15 min. [f] 1 equiv. $B(C_6F_5)_3$/10 equiv. TMA, reaction time 15 min. [g] 1 equiv. $B(C_6F_5)_3$/10 equiv. TiBAl, reaction time 15 min. [h] Mass transport problems may have occurred.

a large excess is needed, render it less attractive. In addition, a prime objective of this study was to reduce the co-catalyst concentration in order to make the catalyst more amenable to polar co-monomers.

In Table 5 the ethylene polymerisation results for neutral and cationic iron and cobalt complexes activated with different co-catalysts are summarised. Generally, under the given conditions, the neutral and cationic iron complexes bearing the 2,6-diisopropylphenyl-bis(imino)pyridine ligand show an activity between 2000 and 2300 g mmol^{-1} h^{-1} bar^{-1} when activated with 100 equiv. MAO. With 1 equiv. $B(C_6F_5)_3$ and 10 equiv. trimethylaluminium (TMA) as co-catalyst, a decrease in activity to 900–1300 g mmol^{-1} h^{-1} bar^{-1} is observed. This may be due to a less efficient scavenging of catalyst poisons in the case of a lower aluminium alkyl concentration.

Very striking is the effect of the different co-catalysts on the polymer properties. Under Schlenk-line conditions with 1 bar ethylene pressure and 100 equiv. MAO as co-catalyst a bimodal molecular weight distribution of the polyethylene is observed. This is the case for neutral and cationic iron complexes. As discussed previously, at low ethylene pressures and relatively high aluminium alkyl concentrations, the rate of chain transfer to aluminium and the rate of β-H transfer can become competitive, leading to the formation of a fully saturated low molecular weight fraction in addition to the high molecular weight vinyl terminated polymer.[10] Upon consumption of the aluminium alkyl, only high molecular weight polyethylene is produced with β-hydride transfer as the main transfer mechanism. As a consequence of the lower aluminium alkyl concentration, with 1 equiv. $B(C_6F_5)_3$/10 equiv. TMA as co-catalyst only high molecular weight polyethylene is produced with a unimodal molecular weight distribution and relatively narrow PDI. Analysis of the chain ends shows an approximate 1 : 1 ratio between saturated and vinyl end-groups indicating that β-hydride transfer is the sole chain termination mechanism. As seen before with MAO as co-catalyst, no effect of different substituents on the acac ligand or of the different counter ions is observed. Entry 24 in Table 5 shows that triisobutylaluminium (TiBAl) in combination with $B(C_6F_5)_3$ is a less efficient co-catalyst for the iron system.

All cationic iron and cobalt acac complexes can be activated with as little as 10 equiv. TMA. Different colour changes upon activation and after stirring for a few minutes indicate a lower stability of the active species in those cases. Addition of 1 equiv. $B(C_6F_5)_3$ prior to the addition of TMA results in a more stable active species. This is illustrated by the fact that both MAO and $B(C_6F_5)_3$/TMA activated solutions remain active after ageing for 10–15 minutes. Complexes activated with TMA alone are only active immediately after activation. Addition of $MeAlCl_2$ to the active catalyst solution, formed using 1 equiv. $B(C_6F_5)_3$/10 equiv. TMA, resulted in no polymerisation activity. This suggests that chloro aluminium alkyl reagents poison iron and cobalt catalysts, which is in line with the very low activities observed when chloro aluminium alkyls are used as co-catalysts for the neutral iron and cobalt complexes **1a** and **1b**.[6,26]

Co-polymerisation of ethylene with polar monomers. The observation that, for the iron and cobalt bis(imino)pyridine catalysts, the presence of one equivalent of acetonitrile or tetrahydrofuran does not inhibit the polymerisation reaction indicates that these catalysts possess good functional group tolerance. This, along with the finding that these cationic pre-catalysts can be activated with very small amounts of alkyl aluminium co-catalyst, are important requirements for hydrocarbon olefin/polar monomer co-polymerisations. Co-polymerisation tests using ethylene and a variety of polar monomers were carried out under Schlenk-line conditions with 1000 equiv. of the polar momoner and the results are summarised in Table 6. Surprisingly, both the neutral pre-catalyst **1a** (activated with 100 equiv. MAO) and the cationic pre-catalyst **5a** (activated with 1 equiv. $B(C_6F_5)_3$/10 TMA) show high polymerisation activities in the presence of 1000 equiv. methyl methacrylate (MMA) or styrene. In the presence of methyl acrylate (MA) or 2-vinyl-1,3-dioxolane (VDO) the activity is significantly reduced. The polymer properties are also affected. The polydispersity of the polymer generated by the neutral dichloride pre-catalyst **1a**, in combination with MAO, is lowered in the presence of polar monomer (see runs 34–36). This could possibly be due to an interaction between the polar group of the co-monomer and trimethyl aluminium (present in MAO), thereby reducing the rate of chain transfer to aluminium.

Analysis by IR and ^{1}H NMR spectroscopy of the polymer products obtained in runs 35, 36 and 38–41 revealed that in all cases, in addition to the signals for polyethylene, minor signals corresponding to the functional group of the co-monomer were present. However, it should be noted that, at low levels of co-monomer incorporation, the detection by IR and NMR

Table 6 Co-polymerisation results of pre-catalysts **1a** and **5a** with various polar olefins

Run	Precatalyst/ μmol	Polar olefin	Yield/g	Activity[b]	M_w[c]	M_n[c]	M_w/M_n[c]	M_{pk}[c]	Saturated ends[d]	Unsaturated ends[d]
34[e]	**1a** (9.4)		5.4[g]	2300	72000	6000	12.1	43000	3.7	0.4
35[e]	**1a** (9.5)	MMA	2.7	1220	200000	59000	3.4	136000	0.6	0.3
36[e]	**1a** (10.0)	MA	2.2	440	137000	34000	4.1	84000	0.7	0
37[f]	**5a** (9.4)		2.6	1100	117000	40000	2.9	88000	0.5	0.4
38[f]	**5a** (10.0)	MMA	4.1[g]	1600	92000	1300	6.8	43000	0.7	0.4
39[f]	**5a** (10.2)	MA	0.7	140	132000	53000	2.5	101000	0.2	0
40[f]	**5a** (10.0)	Styrene	3.1	1220	214000	70000	3.1	111000	0.8	0.2
41[f]	**5a** (9.4)	VDO	0.4	180	218000	70000	3.7	158000	0.6	0.1

[a] General conditions: toluene solvent (100 ml), 1000 equiv. polar olefin, 1 bar ethylene pressure, r.t., reaction time 15 min (except runs 36 and 39; 30 min). [b] g mmol^{-1} h^{-1} bar^{-1}. [c] Determined by GPC at 135 °C. [d] Results from ^{1}H NMR analysis, given per 1000 carbon atoms. [e] 100 equiv. MAO [f] 1 equiv. $B(C_6F_5)_3$/10 equiv. TMA. [g] Mass transport problems may have occurred.

spectroscopy of true co-polymers, as compared to a blend of two homo-polymers, is not straightforward. We therefore employed a procedure[62] of dissolving the crude polymer products obtained in runs 35–36 and 38–41 (Table 6) in hot 1,2,4-trichlorobenzene, followed by precipitation in thf (see experimental). Blank experiments were carried out using homo-polymer mixtures of polyethylene and PMMA, PMA or polystyrene, respectively. IR spectroscopic analysis clearly showed that these mixtures are easily separated via this procedure. In the case of PMA the procedure had to be repeated several times. IR spectroscopic analysis of the purified polymer no longer showed the characteristic absorptions for the polar co-monomers, clearly establishing that in all co-polymerisation experiments a mixture of homo-polymers had been produced, rather than a co-polymer. By comparison of the IR spectra with those of the materials used in the blank experiments, it can be estimated that the amount of polar homo-polymer was generally very low. It is interesting to note that, under similar reaction conditions, but in the absence of ethylene, homo-polymerisation of these polar monomers does not occur.

In the case of other polar monomers such as vinyl acetate, acrolein or acrylonitrile, no polymer is obtained when these polar monomers are added to the activated catalyst solution prior to the addition of ethylene (conditions as in run 38, Table 6). In another series of experiments where these polar monomers were added 90 s after exposure of the activated catalyst to ethylene, *i.e.* after ethylene polymerisation has commenced, only polyethylene was produced; there was no evidence by NMR and IR spectroscopy for polar monomer incorporation.

Conclusion

The synthesis and characterisation of a series of cationic iron and cobalt complexes have been described, all containing the same 2,6-diisopropylphenyl substituted bis(imino)pyridine ligand. Activation with MAO produces highly active ethylene polymerisation catalysts. As seen for the neutral dichloride complexes, the cationic iron complexes show an order of magnitude higher activity than the corresponding cobalt complexes. The formation of cationic pre-catalysts with different acac substituents and different counter ions has no adverse affect on the catalyst activity. In fact, little difference in activity and polymer properties is observed between neutral dichloro, or cationic monochloro or acac pre-catalysts, which leads us to conclude that the active species generated upon activation with MAO, is likely to be the same in all cases and does not contain any of the co-ligands (chloride, acac or acetonitrile). Co-catalysts other than MAO have been tested and co-catalyst concentrations as low as 10 equiv. TMA per metal centre afford efficient ethylene polymerisation catalysts. The resultant materials possess narrower molecular weight distributions than those obtained from neutral dichloride precatalysts where much larger activator concentrations are employed. Co-polymerisation tests with methyl methacrylate (MMA), methyl acrylate (MA), styrene and 2-vinyl-1,3-dioxolane (VDO) were carried out. Both the neutral and the cationic iron complexes are active polymerisation catalysts in the presence of these polar olefins, whereas monomers such as vinyl acetate, acrolein or acrylonitrile deactivate the catalyst. In all co-polymerisation tests no incorporation of the polar monomer into the ethylene chain can be substantiated.

Experimental

General considerations

All manipulations of water and/or moisture sensitive compounds were performed by means of standard high vacuum Schlenk and cannula techniques. Complexes were transferred in a nitrogen filled glove-box and, unless stated otherwise, stored at room temperature. Crystal data were collected on a Siemens P4/PC diffractometer with Cu-Kα radiation. ^{1}H NMR spectra were recorded with a Bruker AC-250 spectrometer. Chemical shifts were referenced to the residual proton signal of the deuterated solvents. Infrared spectra were obtained on a Perkin Elmer 1760X FT-IR spectrometer using thin film samples on NaCl plates. Relative intensities of the IR-bands have been described as w (weak), m (medium), s (strong). UV/VIS spectra were recorded in 10 mm quarz glass cells on a Perkin Elmer Lambda 20 spectrometer. Mass spectra were recorded on either a VG Autospec or a VG Platform II spectrometer. Elemental analysis were performed by the microanalytical services of the Chemistry Departments of Imperial College and the University of North London. GPC and NMR spectroscopic analyses of polyethylene were performed by BP Chemicals at Sunbury. Magnetic moments were determined by the Evans NMR method.[44–47]

Solvents and reagents

Pentane and toluene were dried by passing through a column, filled with commercially available Q-5 reactant (13 wt.% CuO on alumina) and activated alumina (pellets, 3 mm). The following solvents were dried by prolonged reflux over a suitable drying agent under an atmosphere of nitrogen, being freshly distilled prior to use. For diethyl ether and tetrahydrofuran (thf), sodium benzophenone ketyl was used as drying agent, whereas acetonitrile (MeCN) and dichloromethane were dried over calcium hydride. All solvents were used without degassing unless otherwise stated. CD_2Cl_2 was dried over 4 Å molecular sieves. Ethylene was purchased from BOC Gases and used without further purification. Methylacrylate (MA) and methylmethacrylate (MMA) were dried over calcium hydride and vacuum-transferred and degassed prior to use. Styrene (St) and 2-vinyl-1,3-dioxolane (VDO) were dried over 4 Å molecular sieves and distilled and degassed prior to use. The 2,6-bis-[1-(2,6-diisopropylphenylimino)ethyl]pyridine ligand (UV/VIS

(CH_2Cl_2): λ_{max}/nm (ε_{max}/dm^3 mol^{-1} cm^{-1}) = 343 (1400), 279 (11500), 234 (42000)) and the complexes **1a** (UV/VIS (CH_2Cl_2): λ_{max}/nm (ε_{max}/dm^3 mol^{-1} cm^{-1}) = 695 (2500), 289 (7000), 224 (44500)) and **1b** (UV/VIS (CH_2Cl_2): λ_{max}/nm (ε_{max}/dm^3 mol^{-1} cm^{-1}) = 703 (400), 291 (7000), 228 (32000)) were prepared according to published procedures.[10] All other reagents are commercially available and were used without further purification.

Syntheses

2,6-Bis[1-(2,6-diisopropylphenylimino)ethyl]pyridine iron(II) chloride hexafluoroantimonate acetonitrile adduct (2a). Silver hexafluoroantimonate (1.22 g, 2.0 mmol) and **1a** (687 mg, 2.00 mmol) were dissolved in 50 ml MeCN. After stirring at r.t. for 16 h the solution was filtered off and the solvent removed *in vacuo*. The residue was washed with diethyl ether (2 × 30 ml). After drying *in vacuo* a red powder was obtained. Yield: 1.59 g (94%). Crystals suitable for X-ray analysis were grown from a concentrated dichloromethane solution layered with pentane. ^{1}H NMR (250 MHz, CD_2Cl_2, r.t., all peaks appear as broad singlets): δ −13.8 (1H, PyH_p), −13.1 (2H, PhH_p), −8.7 (6H, N=C–*Me*), −2.2 (24H, iPr*Me*), 10.6 (4H, iPrC*H* or PhH_m), 12.4 (4H, PhH_m or iPrC*H*), 100.6 (2H, PyH_m). IR (neat compound): 1617 (m, ν(C=N)), 670 (s, ν(Sb–F)) cm^{-1}. UV/VIS (CH_2Cl_2): λ_{max}/nm (ε_{max}/dm^3 mol^{-1} cm^{-1}) = 540 (400), 298 (6000), 224 (39000). FAB mass spectrum (*m*/*z*): 572 [(M − SbF_6)$^+$ − MeCN]. Anal. Calcd. for $C_{35}H_{46}N_4ClF_6FeSb\cdot0.5CH_2Cl_2$: C, 47.79; H, 5.31; N, 6.28. Found: C, 48.06; H, 5.09; N, 6.39%. μ_{eff} (Evans' NMR method) = 5.4 μ_B.

2,6-Bis[1-(2,6-diisopropylphenylimino)ethyl]pyridine cobalt(II) chloride hexafluoroantimonate acetonitrile adduct (2b). By using the procedure described above and **1b** as the starting complex, a green powder was obtained in 56% yield. Crystals suitable for X-ray analysis were grown from a concentrated dichloromethane solution layered with pentane. ^{1}H NMR (250 MHz, CD_2Cl_2, r.t., all peaks appear as broad singlets): δ −65.9 (2H, PhH_p), −24.9 (12H, iPr*Me*), −11.6 (12H, iPr*Me*), −6.3 (4H, iPrC*H* or PhH_m), 15.7 (6H, N=C–*Me*), 16.9 (4H, PhH_m or iPrC*H*), 50.6 (1H, PyH_p), 125.4 (2H, PynH_m). IR (neat compound): 1618 (w, ν(C=N)), 662 (s, ν(Sb–F)) cm^{-1}. UV/VIS (CH_2Cl_2): λ_{max}/nm (ε_{max}/dm^3 mol^{-1} cm^{-1}) = 647 (200), 293 (8000), 227 (28000). FAB mass spectrum (*m*/*z*): 575 [(M − SbF_6)$^+$ − MeCN]. Anal. Calcd. for $C_{35}H_{46}N_4ClCoF_6Sb\cdot1.5\ CH_2Cl_2$: C, 44.72; H, 5.04; N, 5.71. Found: C, 44.47; H, 5.18; N, 5.36%. μ_{eff} (Evans' NMR method) = 4.6 μ_B.

2,6-Bis[1-(2,6-diisopropylphenylimino)ethyl]pyridine cobalt(II) chloride hexafluoroantimonate tetrahydrofuran adduct (3). Silver hexafluoroantimonate (225 mg, 0.655 mmol) and **1b** (400 mg, 0.654 mmol) were dissolved in 75 ml THF. After stirring for 4 h at r.t. 15 ml dichloromethane were added to solubilise the product. The solution was filtered off and the solvent was removed *in vacuo* to obtain a green powder. Yield: 460 mg (80%). Crystals suitable for X-ray analysis were grown from a concentrated dichloromethane solution layered with pentane. ^{1}H NMR (250 MHz, CD_2Cl_2, r.t., all peaks appear as broad singlets): δ −24.9 (12H, iPr*Me*), −11.9 (12H, iPr*Me*), −6.5 (4H, iPrC*H* or PhH_m), 15.7 (4H, iPrC*H* or PhH_m), 18.0 (6H, N=C–*Me*), 53.2 (1H, PyH_p), 123.7 (2H, PyH_m). IR (neat compound): 1619 (m, ν(C=N)), 660 (s, ν(Sb–F)) cm^{-1}. FAB mass spectrum (*m*/*z*): 575 [(M − SbF_6)$^+$ − THF]. Anal. Calcd. for $C_{37}H_{51}N_3ClOCoF_6Sb$: C 50.27, H 5.82, N 4.75. Found C 50.26, H 5.81, N 4.84%. μ_{eff} (Evans' NMR method) = 4.9 μ_B.

2,6-Bis[1-(2,6-diisopropylphenylimino)ethyl]pyridine iron(II) acetylacetonate hexafluoroantimonate (5a). Silver acetylacetonate (420 mg, 0.49 mmol) and **2a** (102 mg, 0.49 mmol) were dissolved in 30 ml MeCN. After stirring at r.t. for 16 h, the solution was filtered off and the solvent was removed *in vacuo*. The red residue was redissolved in 10 ml dichloromethane and precipitated with 60 ml pentane. The supernatant solution was filtered off and the residue was dried *in vacuo*. Yield: 390 mg (91%). Crystals suitable for X-ray analysis were grown from a concentrated dichloromethane solution layered with pentane. ^{1}H NMR (250 MHz, CD_2Cl_2, r.t., all peaks appear as broad singlets): δ −60.5 (6H, N=C–*Me*), −33.0 (1H, PyH_p), −22.1 (6H, O=C–*Me*), −12.67 (2H, PhH_p), −6.0 (12H, iPr*Me*), −2.8 (12H, iPr*Me*), 2.4 (4H, iPrC*H* or PhH_m), 13.1 (4H, iPrC*H* or PhH_m), 30.5 (1H, O=C–C*H*), 117.3 (2H, PyH_m). IR (neat compound): 1625 (w, ν(C=N)), 1567 (s, ν(C=C) + ν(C=O)), 1522 (s, ν(C=C) + ν(C=O)), 659 (s, ν(Sb–F)) cm^{-1}. UV/VIS (CH_2Cl_2): λ_{max}/nm (ε_{max}/dm^{3}mol^{-1}cm^{-1}) = 560 (500), 296 (11000), 228 (27500). FAB mass spectrum (*m*/*z*): 636 [(M − SbF_6)$^+$], 620 [(M − SbF_6)$^+$ − CH_3]. Anal. Calcd. for $C_{38}H_{50}N_3F_6FeO_2Sb\cdot1\ CH_2Cl_2$: C, 48.93; H, 5.47; N, 4.39. Found: C, 49.11; H, 5.33; N, 4.33%. μ_{eff} (Evans' NMR method) = 5.0 μ_B.

2,6-Bis[1-(2,6-diisopropylphenylimino)ethyl]pyridine cobalt(II) acetylacetonate hexafluoroantimonate (5b). Silver hexafluoroantimonate (640 mg, 1.9 mmol) and **1b** (1.14 g, 1.9 mmol) were dissolved in 50 ml MeCN and stirred at r.t. for one hour. Then a suspension of silver acetylacetonate (384 mg, 1.9 mmol) in 20 ml MeCN was added. After stirring at r.t. for 16 h the solution was filtered off and the solvent was removed *in vacuo*. The residue was washed with diethyl ether and after drying *in vacuo* the product was obtained as a pale green solid. Yield: 1.30 g (78%). By using the procedure described above and **2b** as the starting complex, a green powder was obtained in 53% yield. ^{1}H NMR (250 MHz, CD_2Cl_2, r.t., all peaks appear as broad singlets): δ −73.7 (4H, iPrC*H* or PhH_m), −35.6 (1H, O=C–C*H*), −12.3 (12H, iPr*Me*), −11.6 (12H, iPr*Me*), −9.9 (2H, PhH_p), −9.5 (6H, O=C–*Me*), 10.3 (6H, N=C–*Me*), 12.04 (4H, PhH_m or iPrC*H*), 35.2 (1H, PyH_p), 116.2 (2H, PyH_m). IR (neat compound): 1624 (w, ν(C=N)), 1578 (s, ν(C=C) + ν(C=O)), 1522 (s, ν(C=C) + ν(C=O)), 659 (s, ν(Sb–F)) cm^{-1}. UV/VIS (CH_2Cl_2): λ_{max}/nm (ε_{max}/dm^{3}mol^{-1}cm^{-1}) = 670 (100), 483 (900), 293 (14000), 228 (32000). FAB mass spectrum (*m*/*z*): 639 [(M − SbF_6)$^+$]. Anal. Calcd. for $C_{38}H_{50}N_3CoF_6O_2Sb\cdot2CH_2Cl_2$: C, 45.96; H, 5.21; N, 4.02. Found: C, 45.41; H, 4.93; N, 4.21%. μ_{eff} (Evans' NMR method) = 4.6 μ_B.

2,6-Bis[1-(2,6-diisopropylphenylimino)ethyl]pyridine iron(II) 1,3-bis(trifluoromethyl)-1,3-propanedionate hexafluoroantimonate (6). Sodium 1,3-trifluoromethyl-1,3-propanedionate (46 mg, 0.20 mmol) and **2a** (170 mg, 0.20 mmol) were dissolved in a mixture of 30 ml diethyl ether and 10 ml dichloromethane. After stirring at r.t. for 16 h the solvent was removed *in vacuo* and the residue was extracted with dichloromethane. After removal of the solvent *in vacuo* a purple powder was obtained. Yield: 100 mg (51%). ^{1}H NMR (250 MHz, CD_2Cl_2, r.t., all peaks appear as broad singlets): δ −27.5 (1H, PyH_p), −19.21 (1H, O=C–C*H*), −14.6 (2H, PhH_p), −6.4 (12H, iPr*Me*), −2.2 (12H, iPr*Me*), 6.7 (4H, iPrC*H* or PhH_m), 14.4 (4H, iPrC*H* or PhH_m), 116.8 (2H, PyH_{im}). IR (neat compound): 1625 (w, ν(C=N)), 1552 (w, ν(C=C) + ν(C=O)), 1522 (w, ν(C=C) + ν(C=O), 1206 (s, ν(CF_3), 1147 (s, ν(CF_3)), 660 (s, ν(Sb–F)) cm^{-1}. FAB mass spectrum (*m*/*z*): 744 [(M − SbF_6)$^+$]. Anal. Calcd. for $C_{38}H_{44}N_3F_{12}FeO_2Sb$: C, 46.56; H, 4.52; N, 4.29. Found: C, 46.72; H, 4.48; N, 4.28%. μ_{eff} (Evans' NMR method) = 5.3 μ_B.

2,6-Bis[1-(2,6-diisopropylphenylimino)ethyl]pyridine iron(II) 1,3-diphenyl-1,3-propanedionate hexafluoroantimonate (7). Sodium 1,3-diphenyl-1,3-propanedionate[63] (74 mg, 0.30 mmol) and **2a** (250 mg, 0.30 mmol) were dissolved in 40 ml MeCN. After stirring at r.t. for 16 h the solvent was removed *in vacuo* and the red residue was extracted with dichloromethane. After removing the solvent *in vacuo* a purple powder was obtained. Yield: 170 mg (57%). ^{1}H NMR (250 MHz, CD_2Cl_2, r.t., all

peaks appear as broad singlets): δ −33.77 (1H, PyH_p), −13.7 (2H, PhH_p), −5.5 (12H, iPr*Me*), −1.9 (12H, iPr*Me*), 6.6 (10H, O=C-*Ph*), 12.8 (6H, N=C–*Me*), 22.5 (4H, iPrC*H* or PhH_m), 25.5 (4H, iPrC*H* or PhH_m), 114.0 (2H, PyH_m). IR (neat, cm^{-1}): 1624 (w, ν(C=N)), 1522 (s, ν(C=C) + ν(C=O)), 658 (s, ν(Sb–F)). FAB mass spectrum *m*/*z*): 760 [(M − SbF_6)$^+$]. Anal. Calcd. for $C_{48}H_{54}N_3F_6FeO_2Sb$: C, 57.85; H, 5.46; N, 4.22. Found: C, 57.95; H, 5.33; N, 4.14%. μ_{eff} (Evans' NMR method) = 5.4 μ_B.

2,6-Bis[1-(2,6-diisopropylphenylimino)ethyl]pyridine iron(II) acetylacetonate tetraphenylborate (8). Silver acetylacetonate (108 mg, 0.52 mmol) and **1a** (316 mg, 0.52 mmol) were dissolved in 30 ml MeCN. After stirring at r.t. for 1 h, the solution was filtered into a solution of 188 mg (0.55 mmol) sodium tetraphenylborate in 20 ml MeCN. Further extractions of the dark residue with MeCN were also added. After stirring at r.t. for 16 h, the solvent was removed *in vacuo* and the red residue was extracted with dichloromethane. The solution was concentrated *in vacuo* to 5 ml. The product was precipitated by addition of pentane. After removing the supernatant solution and drying *in vacuo* a red powder was obtained. Yield: 351 mg (71%). ^{1}H NMR (250 MHz, CD_2Cl_2, r.t., all peaks appear as broad singlets): δ −61.5 (6H, N=C–*Me*), −34.5 (1H, PyH_p), −22.7 (6H, O=C–*Me*), −12.9 (2H, PhH_p), −6.0 (12H, iPr*Me*), −2.9 (12H, iPr*Me*), 2.3 (4H, PhH_m or iPrC*H*), 7.0 (4H, BPh*H*), 7.4 (8H, BPh*H*), 8.5 (8H, BPh*H*), 13.1 (4H, iPrC*H* or PhH_m), 30.4 (1H, O=C–C*H*), 117.8 (2H, PyH_m). IR (neat compound): 1621 (w, ν(C=N)) cm^{-1}. FAB mass spectrum (*m*/*z*): 636 [(M − B(C_6H_5)$_4$)$^+$]. Anal. Calcd. for $C_{62}H_{70}N_3BFe$: C, 77.90; H, 7.38; N, 4.40. Found: C, 77.90; H, 7.40; N, 4.63. μ_{eff} (Evans' NMR method) = 5.1 μ_B.

Magnetic susceptibility

According to the NMR method described by Evans,[44–47] a solution of the compound (≈ 3 mg) in a mixture of dichloromethane-d_2/cyclohexane (95/5 v/v) was prepared in a 1.0 ml volumetric flask. A portion of this solution was transferred into a melting point capillary tube that was sealed with PTFE-tape and dropped into a NMR tube containing the dichloromethane-d_2/cyclohexane (95/5 v/v) mixture. The chemical shift difference of the cyclohexane signal between the inner and the outer tubes was measured at room temperature. From this difference in the chemical shift the molar susceptibility χ_M and the magnetic moment μ_{eff} can be calculated with equations (1) and (2) (given in S.I. units).

$$\chi_M = \frac{3 \cdot \Delta f}{1000 \cdot f \cdot c} \quad (1)$$

$$\mu_{eff} = \sqrt{\frac{3k}{N_0 \cdot \mu_0 \cdot \mu_B^2} \cdot T \cdot \chi_M} = 798\sqrt{T \cdot \chi_M} \quad (2)$$

where: χ_M is the molar susceptibility of the sample in m^3 mol, Δ: is the difference in the chemical shift of a set of protons in Hz, : is the frequency of operation of the spectrometer in Hz, *c* is the concentration of the sample in mol dm^{-3}, *T* is the temperature in *K*.

General polymerisation procedures

High pressure tests in a 1 l steel autoclave. A 1 l stainless steel reactor was baked under nitrogen flow for at least 1 h at >85 °C and subsequently cooled to the temperature of polymerisation. Isobutane (0.5 l) and triisobutylaluminium (2.0 ml, 1.0 M in hexane) were introduced into the reactor and stirred at the reaction temperature for at least 1 h. Ethylene was introduced into the reactor by backpressure of nitrogen. The catalyst solution was prepared by dissolving the pre-catalyst in toluene and adding MAO (10 wt% in toluene) in a Schlenk-tube. An aliquot of this solution was then injected into the reactor under nitrogen pressure. The reactor pressure was maintained constant throughout the polymerisation run by computer-controlled addition of ethylene. The polymerisation time was 60 minutes. Venting off all volatiles terminated the runs, the reactor contents were isolated, washed with aqueous HCl and methanol, and dried in a vacuum oven at 50 °C.

High pressure tests in 500 ml Fisher–Porter glass reaction vessels. A 500 ml glass bottle with a stainless steel headset containing a mechanical stirrer and an injection valve was evacuated and flushed with nitrogen 3 times before it was filled with toluene (250 ml). The catalyst solution was prepared by dissolving the pre-catalyst in toluene and adding MAO (10 wt% in toluene) in a Schlenk-tube. An aliquot of this solution was then injected under nitrogen pressure. Ethylene was introduced into the reactor, and the reactor pressure was maintained at 5 bar throughout the polymerisation run by addition of ethylene. The polymerisation time was 15 minutes. Releasing the ethylene pressure and adding aqueous HCl and methanol terminated the runs. The solid PE was recovered by filtration, washed with methanol, and dried in a vacuum oven at 50 °C.

Schlenk-line 1 bar ethylene tests. The pre-catalyst was dissolved in toluene (120 ml) and a solution of B(C_6F_5)$_3$ in toluene and trimethylaluminium (2.0 M in toluene) was added. The Schlenk tube was purged with ethylene, and the contents were magnetically stirred and maintained under ethylene (1 bar) throughout the polymerisation run. The polymerisation time was 15 minutes. Releasing the ethylene pressure and adding aqueous HCl and methanol terminated the runs. The solid PE was recovered by filtration, washed with methanol, and dried in a vacuum oven at 60 °C.

General co-polymerisation procedures

Schlenk-line 1 bar ethylene tests. The pre-catalyst was dissolved in toluene (120 ml) and a solution of B(C_6F_5)$_3$ in toluene and trimethylaluminium (2.0 M in toluene) was added. The polar monomer (typically 1000 equivalents) was added *via* syringe. The Schlenk tube was purged with ethylene, and the contents were magnetically stirred and maintained under ethylene (1 bar) throughout the polymerisation run. The polymerisation time was 15 minutes. Releasing the ethylene pressure and adding aqueous HCl and methanol terminated the runs. The solid polymer was recovered by filtration, washed thoroughly with methanol, and dried in a vacuum oven at 60 °C. The crude polymer product was subsequently dissolved in hot 1,2,4-trichlorobenzene and the hot solution poured into a tenfold excess of tetrahydrofuran at room temperature. The precipitated polymer was collected by filtration, washed with thf and dried in a vacuum oven at 60 °C.

X-Ray crystallography

Table 7 provides a summary of the crystal data, data collection and refinement parameters for compounds **2a**, **2b**, **3**, **4i**, **4ii**, **5a**, **6i**, **6ii** and **7**.

CCDC reference numbers 168887–168895.

See http://www.rsc.org/suppdata/dt/b1/b106614p/ for crystallographic data in CIF or other electronic format.

Acknowledgements

The authors are grateful to BP Chemicals Ltd. for financial support. Dr J. Boyle and Dr. G. Audley are thanked for GPC and NMR measurements. Dr P. Maddox and Prof. D. Goodgame are thanked for helpful discussions.

Table 7 Crystal data, data collection and refinement parameters for compounds **2a**, **2b**, **3**, **4i**, **4ii**, **5a**, **6i**, **6ii** and **7** [a]

Data	**2a**	**2b**	**3**	**4i**	**4ii**	**5a**	**6i**	**6ii**	**7**
Formula	$[C_{35}H_{46}N_4ClFe]$-$[SbF_6]\cdot CH_2Cl_2\cdot 0.5C_5H_{12}$	$[C_{35}H_{46}N_4ClCo]$-$[SbF_6]\cdot 1.5CH_2Cl_2$	$[C_{37}H_{51}N_3OClCo]$-$[SbF_6]\cdot 2CH_2Cl_2$	$[C_{33}H_{45}N_3OClFe]$-$[SbF_6]\cdot 2CH_2Cl_2$	$[C_{33}H_{45}N_3OClFe]$-$[SbF_6]\cdot 1.5CH_2Cl_2\cdot H_2O$	$[C_{38}H_{50}N_3O_2Fe]$-$[SbF_6]\cdot 2CH_2Cl_2$	$[C_{38}H_{44}N_3O_2F_6Fe]$-$[SbF_6]$	$[C_{38}H_{44}N_3O_2F_6Fe]$-$[SbF_6]$	$[C_{48}H_{54}N_3O_2Fe]$-$[SbF_6]$
Formula weight	970.8	980.3	1053.8	996.6	972.2	1042.3	980.4	980.4	996.5
Colour, habit	Deep red needles	Orange/red prisms	Green prisms	Deep red needles	Deep red prisms	Orange/red prisms	Red blocks	Orange plates	Red platy needles
Crystal size/mm	0.40 × 0.37 × 0.27	0.37 × 0.33 × 0.17	0.83 × 0.33 × 0.33	0.90 × 0.07 × 0.06	0.30 × 0.27 × 0.20	0.77 × 0.73 × 0.33	0.43 × 0.43 × 0.17	0.57 × 0.37 × 0.07	0.73 × 0.12 × 0.05
Crystal system	Monoclinic	Monoclinic	Triclinic	Monoclinic	Triclinic	Monoclinic	Monoclinic	Triclinic	Monoclinic
Space group	*C*2/*c* (no. 15)	*C*2/*c* (no. 15)	$P\bar{1}$ (no. 2)	$P2_1/c$ (no. 14)	$P\bar{1}$ (no. 2)	$P2_1/c$ (no. 14)	$P2_1/c$ (no. 14)	$P\bar{1}$ (no. 2)	$P2_1/n$ (no. 14)
T/K	293	293	173	203	293	293	293	293	193
a/Å	25.925(2)	25.879(5)	9.982(3)	9.938(2)	10.075(2)	15.005(2)	12.518(3)	9.214(2)	12.464(1)
b/Å	10.063(1)	10.073(2)	14.094(3)	24.269(3)	13.265(3)	16.903(2)	37.750(4)	12.567(2)	17.145(1)
c/Å	36.759(3)	36.573(4)	17.000(3)	18.711(4)	18.925(3)	18.815(2)	9.275(2)	19.096(2)	21.572(1)
α/°	—	—	88.86(1)	—	84.22(2)	—	—	87.53(1)	—
β/°	92.55(1)	93.01(1)	86.75(2)	104.90(2)	78.89(2)	94.95(1)	97.10(1)	78.49(1)	90.44(1)
γ/°	—	—	83.77(2)	—	68.34(2)	—	—	83.31(1)	—
V/Å^3	9580(1)	9521(3)	2374(1)	4361(1)	2305.4(7)	4754.3(9)	4349(1)	2151.5(6)	4609.6(5)
Z	8	8	2	4	2	4	4	2	4
D_c/g cm^{-3}	1.346	1.368	1.474	1.518	1.400	1.456	1.497	1.513	1.436
Radiation used	Cu-Kα	Cu-Kα	Mo-Kα	Cu-Kα [b]	Mo-Kα	Mo-Kα	Mo-Kα	Mo-Kα	Cu-Kα [b]
μ/mm^{-1}	8.89	9.73	1.26	10.9	1.19	1.16	1.04	1.05	7.72
θ range/deg	2.4–60.0	2.4–57.1	1.9–25.0	3.1–60.0	2.0–25.0	1.8–25.0	2.0–22.5	1.9–25.0	3.3–60.0
No. of unique reflections measured	6994	6327	8361	6269	8112	8301	5676	7553	6786
observed, $\lvert F_o\rvert > 4\sigma(\lvert F_o\rvert)$	3810	3496	6404	3729	4073	4802	3821	4293	5456
Absorption correction	Ellipsoidal	Ellipsoidal	—	Empirical	Ellipsoidal	Ellipsoidal	—	—	Ellipsoidal
Max., min. transmission	0.11, 0.02	0.23, 0.09	—	0.62, 0.14	0.82, 0.74	0.55, 0.49	—	—	0.57, 0.36
No. of variables	542	509	551	469	519	550	514	538	527
R_1, wR_2 [c]	0.081, 0.190	0.076, 0.178	0.052, 0.128	0.065, 0.151	0.082, 0.185	0.066, 0.151	0.056, 0.120	0.076, 0.163	0.048, 0.116

[a] Details in common: graphite monochromated radiation, *ω*-scans, Siemens P4 diffractometer, refinement based on F^2. [b] Rotating anode source. [c] $R_1 = \Sigma\lvert\lvert F_o\rvert - \lvert F_c\rvert\rvert/\Sigma\lvert F_o\rvert$; $wR_2 = \{\Sigma[w(F_o^2 - F_c^2)^2]/\Sigma[w(F_o^2)^2]\}^{1/2}$; $w^{-1} = \sigma^2(F_o^2) + (aP)^2 + bP$.

References

1 G. J. P. Britovsek, V. C. Gibson and D. F. Wass, *Angew. Chem., Int. Ed.*, 1999, **38**, 428.
2 S. D. Ittel, L. K. Johnson and M. Brookhart, *Chem. Rev.*, 2000, **100**, 1169.
3 S. Mecking, *Angew. Chem., Int. Ed.*, 2001, **40**, 534.
4 G. J. P. Britovsek, V. C. Gibson, B. S. Kimberley, P. J. Maddox, S. J. McTavish, G. A. Solan, A. J. P. White and D. J. Williams, *Chem. Commun.*, 1998, 849.
5 B. L. Small, M. Brookhart and A. M. A. Bennett, *J. Am. Chem. Soc.*, 1998, **120**, 4049.
6 G. J. P. Britovsek, B. A. Dorer, V. C. Gibson, B. S. Kimberley, G. A. Solan, *World Pat*., *WO 99/12981* (BP Chemicals Ltd.), 1999; G. J. P. Britovsek, B. A. Dorer, V. C. Gibson, B. S. Kimberley and G. A. Solan, *Chem. Abstr.*, 1999, **130**, 252793.
7 A. M. A. Bennett, *World Pat*., *WO 98/27124* (DuPont), 1998; A. M. A. Bennett, *Chem. Abstr.*, 1998, **129**, 122973.
8 V. C. Gibson and D. F. Wass, *Chem. Br.*, 1999, **35**, 20.
9 A. M. A. Bennett, *CHEMTECH*, 1999, July, 24.
10 G. J. P. Britovsek, M. Bruce, V. C. Gibson, B. S. Kimberley, P. J. Maddox, S. Mastroianni, S. J. McTavish, C. Redshaw, G. A. Solan, S. Strömberg, A. J. P. White and D. J. Williams, *J. Am. Chem. Soc.*, 1999, **121**, 8728.
11 B. L. Small and M. Brookhart, *J. Am. Chem. Soc.*, 1998, **120**, 7143.
12 G. J. P. Britovsek, S. Mastroianni, G. A. Solan, S. P. D. Baugh, C. Redshaw, V. C. Gibson, A. J. P. White, D. J. Williams and M. R. J. Elsegood, *Chem. Eur. J.*, 2000, **6**, 2221.
13 G. J. P. Britovsek, V. C. Gibson, S. Mastroianni, D. C. H. Oakes, C. Redshaw, G. A. Solan, A. J. P. White and D. J. Williams, *Eur. J. Inorg. Chem.*, 2001, 431.
14 P. T. Matsunaga, *World Pat.*, *WO 99/57159* (Exxon Chemical Patents Inc.), 1999; P. T. Matsunaga, *Chem. Abstr.*, 1999, **131**, 351802.
15 S. Al-Benna, M. J. Sarsfield, M. Thornton-Pett, D. L. Ormsby, P. J. Maddox, P. Brès and M. Bochmann, *J. Chem. Soc., Dalton Trans.*, 2000, 4247.
16 D. M. Dawson, D. A. Walker, M. Thornton-Pett and M. Bochmann, *J. Chem. Soc., Dalton Trans.*, 2000, 459.
17 L. S. Moody, P. B. Mackenzie, C. M. Killian, G. G. Lavoie, J. A. Ponasik Jr., A. G. M. Barrett, T. W. Smith, J. C. Pearson, *World Pat.*, *WO 00/50470* (Eastman Chemical Company), 2000; L. S. Moody, P. B. Mackenzie, C. M. Killian, G. G. Lavoie, J. A. Ponasik Jr., A. G. M. Barrett, T. W. Smith and J. C. Pearson, *Chem. Abstr.*, 2000, **133**, 208316.
18 R. Engehausen, W. Nentwig, P. Schertl, M. Arndt-Rosenau, O. Pyrlik, M. Guillemot, *Eur. Pat*., *EP1044992* (Bayer Aktiengesellschaft), 2000; R. Engehausen, W. Nentwig, P. Schertl, M. Arndt-Rosenau, O. Pyrlik and M. Guillemot, *Chem. Abstr.*, 2000, **133**, 310282.
19 K. Nomura, W. Sidokmai and Y. Imanishi, *Bull. Chem. Soc. Jpn.*, 2000, **73**, 599.
20 D. D. Devore, S. S. Feng, K. A. Frazier, J. T. Patton, *World Pat.*, *WO 00/69923* (Dow Chemical Company), 2000; D. D. Devore, S. S. Feng, K. A. Frazier and J. T. Patton, *Chem. Abstr*., 2000, **134**, 5263.
21 K. Kreischer, J. Kipke, M. Bauerfeind and J. Sundermeyer, *Z. Anorg. Allg. Chem.*, 2001, **627**, 1023.
22 L. S. Boffa and B. M. Novak, *Chem. Rev.*, 2000, **100**, 1479.
23 A. Yamamoto, *J. Chem. Soc., Dalton Trans.*, 1999, 1027.
24 A. Yamamoto, *J. Polym. Sci. A*, 1975, **9**, 931.
25 A. Yamamoto, *J. Organomet. Chem.*, 1986, **300**, 347.
26 K. R. Kumar and S. Sivaram, *Macromol. Chem. Phys.*, 2000, **201**, 1513.
27 J. F. van Baar, P. A. Schut, A. D. Horton, T. Dall'occo, G. M. M. van Kessel, *World Pat*., *WO 00/35974*, (Montell Technology Company bv), 2000; J. F. van Baar, P. A. Schut, A. D. Horton, T. Dall'occo and G. M. M. van Kessel, *Chem. Abstr.*, 1999, **133**, 59218.
28 E. A. H. Griffiths, G. J. P. Britovsek, V. C. Gibson and I. R. Gould, *Chem. Commun.*, 1999, 1333.
29 L. Deng, P. Margl and T. Ziegler, *J. Am. Chem. Soc.*, 1999, **121**, 6479.
30 T. Kauffmann, B. Laarmann, D. Menges and G. Neiteler, *Chem. Ber.*, 1992, **125**, 163.
31 T. Kauffmann, *Angew. Chem., Int. Ed. Engl.*, 1996, **35**, 386.
32 W. K. Wong, K. W. Chiu, G. Wilkinson, A. J. Howes, M. Motevalli and M. B. Hursthouse, *Polyhedron*, 1985, **4**, 603.
33 W. Lau, J. C. Huffman and J. K. Kochi, *Organometallics*, 1982, **1**, 155.
34 Y. Kubo, L. Sun Pu, A. Yamamoto and S. Ikeda, *J. Organomet. Chem.*, 1975, **84**, 369.
35 T. Ikariya and A. Yamamoto, *J. Chem. Soc., Chem. Commun.*, 1974, 720.
36 E. L. Dias, M. Brookhart and P. S. White, *Organometallics*, 2000, **19**, 4995.
37 G. J. P. Britovsek, V. C. Gibson, and S. K. Spitzmesser, *World Pat.*, *WO 00/69869* (BP Chemicals), 2000; G. J. P. Britovsek, V. C. Gibson and S. K. Spitzmesser, *Chem. Abstr.*, 2001, **134**, 5260.
38 V. C. Gibson, M. Humphries, K. P. Tellmann, D. F. Wass, A. J. P. White and D. J. Williams, *Chem. Commun.*, 2001, 2252.
39 D. P. Riley, J. A. Stone and D. H. Busch, *J. Am. Chem. Soc.*, 1977, **99**, 767.
40 P. N. Jagg, P. F. Kelly, H. S. Rzepa, D. J. Williams, J. D. Woollins and W. Wylie, *J. Chem. Soc., Chem. Commun.*, 1991, 942.
41 P. A. Cameron, V. C. Gibson, C. Redshaw, J. A. Segal, G. A. Solan, A. J. P. White and D. J. Williams, *J. Chem. Soc., Dalton Trans.*, 2001, 1472.
42 K. Shelly, T. Bartczak, W. R. Scheidt and C. A. Reed, *Inorg. Chem.*, 1985, **24**, 4325.
43 J. -T. Ahlemann, H. W. Roesky, R. Murugavel, E. Parisini, M. Noltemeyer, H.-G. Schmidt, O. Müller, R. Herbst-Irmer, L. N. Markovskii and Y. G. Shermolovich, *Chem. Ber.*, 1997, **130**, 1113.
44 D. F. Evans, *J. Chem. Soc.*, 1959, 2003.
45 D. F. Evans, G. V. Fazakerley and P. R. F. Phillips, *J. Chem. Soc. A*, 1971, 1931.
46 H. D. Crawford and J. Swanson, *J. Chem. Educ.*, 1971, **48**, 382.
47 D. H. Grant, *J. Chem. Educ.*, 1995, **72**, 39.
48 J. -N. Pédeutour, D. Coevoet, H. Cramail and A. Deffieux, *Macromol. Chem. Phys.*, 1999, **200**, 1215.
49 U. Wieser and H.-H. Brintzinger, in *Organometallic Catalysts and Olefin Polymerization (Catalysts for a New Millenium)*, ed. R. Blom, A. Follestad, E. Rytter, M. Tilset and M. Ystenes, Springer Verlag, Berlin, 2001, p. 3.
50 F. Peruch, H. Cramail and A. Deffieux, *Macromolecules*, 1999, **32**, 7977.
51 P. Krumholz, *Inorg. Chem.*, 1965, **4**, 612.
52 B. de Bruin, E. Bill, E. Bothe, T. Weyhermüller and K. Wieghardt, *Inorg. Chem.*, 2000, **39**, 2936.
53 D. Lin-Vien, N. Colthup, W. Fateley and J. G. Graselli, *Infrared and Raman Characteristic Frequencies of Organic Molecules*, Academic Press, San Diego, CA, 1991.
54 K. Nakamoto, *Infrared and Raman Spectra of Inorganic Coordination Compounds*, Wiley, New York, 1989.
55 J. D. Curry, M. A. Robinson and D. H. Busch, *Inorg. Chem.*, 1967, **6**, 1570.
56 P. E. Figgins and D. H. Busch, *J. Phys. Chem. A.*, 1961, **65**, 2236.
57 D. A. Thornton, *Coord. Chem. Rev.*, 1990, **104**, 173.
58 S. Kawaguchi, *Coord. Chem. Rev.*, 1986, **70**, 51.
59 S. Komiya, M. Katoh, T. Ikariya, R. H. Grubbs, T. Yamamoto and A. Yamamoto, *J. Organomet. Chem.*, 1984, **260**, 115.
60 C. J. Pouchert, *The Aldrich Library of Infrared Spectra*, Aldrich Chemical Company Inc., Milwaukee, WI, 1970.
61 A. I. Popov, A. V. Scharabarin, V. F. Sukhoverkhov and N. A. Tchumaevsky, *Z. Anorg. Allg. Chem.*, 1989, **576**, 242.
62 G. Desurmont, M. Tanaka, Y. Li, H. Yasuda, T. Tokimitsu, S. Tone and A. Yanagase, *J. Polym. Sci. A*, 2000, **38**, 4095.
63 H. D. Murdoch and D. C. Nonhebel, *J. Chem. Soc.*, 1962, 2153.